Available online at www.sciencedirect.com
ScienceDirect
Synthetic Metals 157 (2007) 670–677
SYNTHETIC METALS
www.elsevier.com/locate/synmet

Theoretical study of inelastic X-ray scattering spectra for organic materials: Molecular excitation coupled with molecular exciton descriptions

Li Ping Chen [a], Yuanping Yi [a], Qikai Li [a], Zhigang Shuai [a,*], Ke Yang [b], Dong Lai Feng [b]

[a] *Key Laboratory of Organic Solids, Beijing National Laboratory for Molecular Sciences (BNLMS), Institute of Chemistry, Chinese Academy of Sciences, 100080 Beijing, China*
[b] *Department of Physics, Fudan University, 200433 Shanghai, China*

Accepted 12 July 2007
Available online 4 September 2007

Abstract

Inelastic X-ray scattering (IXS) spectrum provides a powerful tool to investigate the electronic structure of organic materials, in complimentary to the conventional optical spectra. Starting from a single molecule, then a dimer, and finally a cluster of molecular aggregate, we developed a Frenkel exciton model to describe the IXS process based on the quantum chemical calculations for the molecular excitations in the organic crystal of open-ring photomerocyanine form of spirooxazine (Py-SO). It is shown that the quantum chemical calculation combined with Frenkel exciton model can well describe the experimental measurements in terms of (i) the overall features of the IXS spectra from 2 to 10 eV, (ii) the dispersion behavior of the lowest exciton band, and (iii) the momentum-transfer dependence of the peak intensity. The roles of molecular excited state and the intermolecular interactions have been discussed for the IXS spectra.

Keywords: Py-SO; Inelastic X-ray scattering spectrum; Frenkel exciton model

1. Introduction

Semiconductors based on organic materials are of great interest due to a wide range of potential application in devices, such as organic light-emitting diodes [1,2], field effect transistors [2,3], organic solar cells [4], or optical converters [5]. Great effort has been invested on designing new functional materials with special optical properties. Understanding the electronic properties is very important for designing new functional materials, since they are directly related to processes such as light absorption and emission, charge transport, photoconductivity, or exciton formation and transfer. In addition, intermolecular interaction plays an important role in determining the properties of organic materials [6].

The conventional optical spectra can probe the excitation processes, but with nearly zero momentum transfer. More information about the electronic states of the materials in momentum space can be obtained if both energy and momentum can be transferred in the excitation process. This can be achieved, for instance, by electron-energy-loss spectrum (EELS) or inelastic X-ray scattering (IXS). EELS has been applied to investigate π-conjugated molecules [7], where the excitons are delocalized, and the information of low q is sufficient for the understanding of the structure of excitons. However, for complex organic molecules, the excitons are localized and the information of high q is required. EELS cannot work well at high q due to low intensity ($\sim q^{-4}$) and multiple scattering effects. There are no such problems for IXS, and it can generate reliable information at high q. Therefore, IXS is particularly advantageous for studying excitons in complex organic molecules. IXS has been proven to be a powerful tool in studying inorganic system [8]. It helps to understand, for example, the metal–insulator transition [9], plasmon excitations [10], and the band gap [11]. Recently, Yang

* Corresponding author.
E-mail addresses: zgshuai@iccas.ac.cn (Z. Shuai), dlfeng@fudan.edu.cn (D.L. Feng).

0379-6779/$ – see front matter © 2007 Elsevier B.V. All rights reserved.
doi:10.1016/j.synthmet.2007.07.003

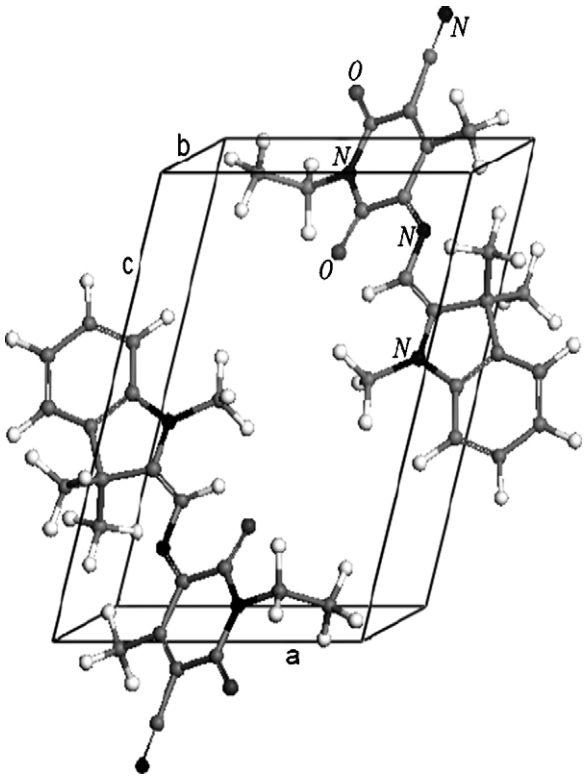

Fig. 1. Crystal structure of Py-SO with the lattice parameters $a = 8.356$ Å, $b = 9.510$ Å, $c = 12.096$ Å, $\alpha = 89.93°$, $\beta = 75.58°$, $\gamma = 81.92°$ at room temperature.

et al. [12] have first applied the IXS technique to study a complex organic molecular crystal of open-ring photomerocyanine form of spirooxazine (Py-SO), which exhibits alkali-induced-chromism and thermochromism in alkali medium [13]. Fig. 1 shows a unit cell of Py-SO crystal. The experimental IXS spectra of momentum-transfer q along the a axis after removing the quasi-elastic Rayleigh background are depicted in Fig. 2(a and b). We can see three main features I–III at 2.2 eV, 4.6 eV and 6.6 eV, respectively. For feature I, an energy dispersion of

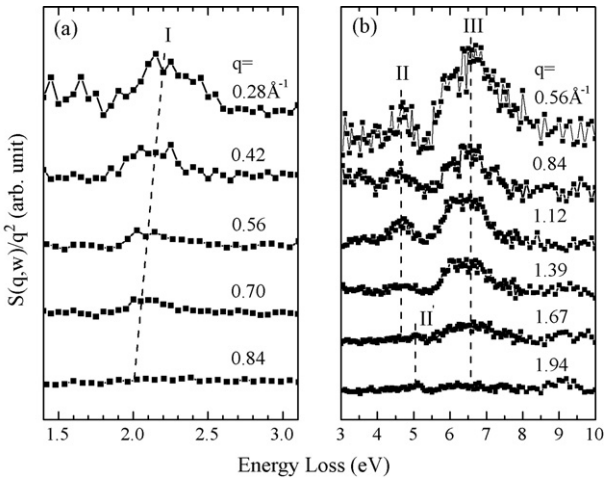

Fig. 2. (a and b) The experimental IXS spectra of Py-SO with momentum-transfer q along the a axis with elastic line removed. Main features are shown by dashed lines.

130 meV is observed when q goes from 0.28 Å^{-1} to 0.70 Å^{-1}. While feature II turns out to be invisible at large q, a small feature II′ at 5.0 eV appears. A broad feature beyond 8 eV can also be observed.

The experimental results and some of the theoretical results have been published in a recent letter [12]. The primary interest of this work is to give a more detailed description for the theoretical approach for the quantum chemical simulations of the IXS spectra, in close comparison with the experiment, to reveal the natures of both the molecular excitation and exciton structures in the organic materials. We first carry out a quantum chemical calculation for a single Py-SO molecule. Then we take a dimer with the shortest separation in the Py-SO crystal to fully consider the effect of intermolecular interaction. Finally, we cut a piece of a cluster from the Py-SO crystal, which is investigated in a simple Frenkel exciton model.

2. Theoretical methodology and results

2.1. Monomer

The chemical structure of a single Py-SO molecule with main atoms labeled is shown in Fig. 3(a). The geometry of the molecule is optimized by semiempirical AM1 (Austin Model 1) method as implemented in the AMPAC package [14], which provides good results for the geometries of organic molecules. The excitation energies and the momentum dependence transition-matrix elements is calculated based upon the semiempirical intermediate neglect of differential overlap method as parameterized by Zerner et al. (ZINDO) [15]. The Mataga–Nishimoto potential [16] is used to describe the Coulomb repulsion terms. We note that the excited state calculation is still a big challenge both for chemistry and physics. The state-of-the-art time-dependent density functional theory (TDDFT) is the

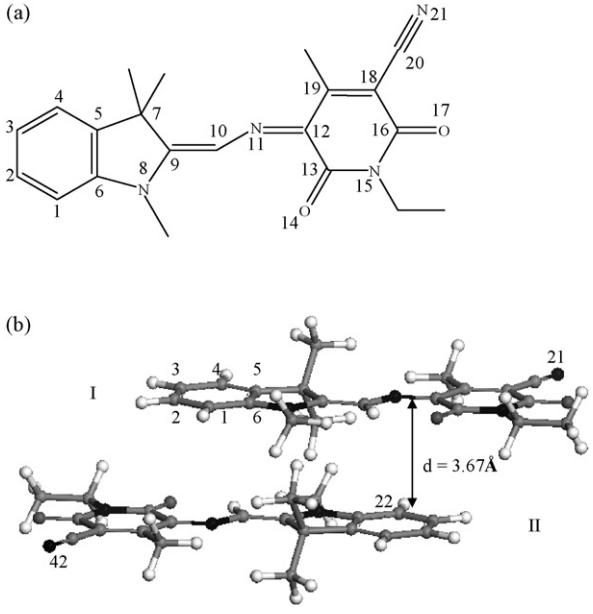

Fig. 3. (a) The chemical structure of a single Py-SO molecule. (b) A dimer with the shortest separation in Py-SO crystal.

most commonly employed approach to describe the low-lying excited states. However, the numerical calculations performed by Hutchison, Ratner and Marks indicated that the standard deviation of TDDFT is even larger than that of ZINDO for a set of 60 organic molecules in terms of the lowest-lying excited state when comparing with the experiments [17]. TDDFT also fails to describe the even-parity excited state ($2A_g$ state) and the charge-transfer excitation [18]. Thus, we opt to the ZINDO Hamiltonian.

The simplest electron–electron correlation effects can be included via a single configuration interaction (SCI) approximation through the electron–hole attraction, where the singlet exciton wave function is expressed as

$$\Psi^{\mathrm{e}} = \frac{1}{\sqrt{2}}\sum_{ia} Z^{e}_{ia}(a^{+}_{\uparrow}i_{\uparrow} + a^{+}_{\downarrow}i_{\downarrow})|0\rangle \tag{1}$$

where $|0\rangle$ is the Hartree–Fock self-consistent Slater determinant for the molecular ground state; i (a^{+}) represents annihilating (creating) an electron in the occupied (unoccupied) molecular orbital, and Z^{e}_{ia} is the linear combination coefficient for the eth excited state. The plus sign in Eq. (1) represents singlet ($S=0$). Thus the spatial representation of the electron–hole wave function can be written as

$$\Psi^{\mathrm{e}}(x_{\mathrm{e}}, x_{\mathrm{h}}) = \sum_{ia} Z^{e}_{ia}\phi_i(x_{\mathrm{h}})\phi_a(x_{\mathrm{e}}) \tag{2}$$

where x_{e} (x_{h}) is the electron (hole) coordinate and ϕ is the molecular orbital wave function. The electron–hole wave function in Eq. (2) has been successfully applied to analyze the charge separation for molecular excitations [19,20] in light-emitting polymer.

The dynamic structure factor characterizing the IXS process is given by [21]:

$$S(q,\omega) = 2\pi\sum_{f}\left|\langle f|\sum_{n=1}^{N} e^{-i\vec{q}\cdot\vec{r}_n}|i\rangle\right|^2 \delta(E_f - E_i - \hbar\omega) \tag{3}$$

where i (f) refers to the initial (final) state, and E_i (E_f) is the energy of the corresponding state. q and $\hbar\omega$ are the momentum transfer and the energy loss, respectively. The summation of index n runs over all the electrons. Note that the structure factor operator is a one-body quantity. Under the SCI approximation, namely, the initial state being Hartree–Fock Slater determinant $|0\rangle$ and the final state $|e\rangle$ being described by Eq. (1), the expectation value in Eq. (3) can be obtained as

$$\langle e|\sum_{n} e^{-i\vec{q}\cdot\vec{r}_n}|0\rangle = \sqrt{2}\sum_{ia} Z^{e}_{ia}\int \mathrm{d}\vec{r}\phi^{*}_{a}(\vec{r})\, e^{-i\vec{q}\cdot\vec{r}}\phi_i(\vec{r}) \tag{4}$$

The molecular orbital is expressed as a linear combination of atomic orbitals. So the evaluation of Eq. (4) invloves basically the integral of the following type:

$$\langle\varphi_\mu(\vec{r}-\vec{R}_\mu)|e^{-i\vec{q}\cdot\vec{r}}|\varphi_\nu(\vec{r}-\vec{R}_\nu)\rangle \tag{5}$$

where φ_μ and φ_ν are atomic orbitals centered at nucleus $\vec{R}_\mu$ and $\vec{R}_\nu$, respectively. By applying the zero differential overlap (ZDO) approximation, Eq. (5) is reduced to

$$e^{-i\vec{q}\cdot\vec{R}_\mu}\int \varphi_\mu(\vec{r}')e^{-i\vec{q}\vec{r}'}\varphi_\nu(\vec{r}')\,\mathrm{d}\vec{r}' \approx e^{-i\vec{q}\cdot\vec{R}_\mu}\delta_{\mu\nu} \tag{6}$$

Then Eq. (4) can be recast into:

$$\langle e|\sum_{n} e^{-i\vec{q}\cdot\vec{r}_n}|0\rangle = \sqrt{2}\sum_{ia} Z^{e}_{ia}\sum_{\mu} C^{a*}_{\mu}C^{i}_{\mu}e^{-i\vec{q}\cdot\vec{R}_\mu} \tag{7}$$

where $C^{i(a)}_{\mu}$ is the linear combination coefficient of the μth atomic orbital for the ith (ath) molecular orbital. Finally, the calculated IXS spectra are obtained by a Gaussian broadening of the δ function with a broadening factor of 170 meV, which is the energy resolution in the IXS experiment.

The calculated IXS spectra for the monomer are shown in Fig. 4, which well reproduce the momentum dependence of the experimentally measured dynamic structure factor. For instances, there are several features, labeled as A, B, B′, C and D. The calculated features A–C at about 2.64 eV, 4.6 eV and 5.0 eV have one to one correspondence with the experimental features I–III (see Fig. 2). Similarly, a small feature B′ around 5.0 eV also appears at high q while feature B disappears. However, the experimentally observed energy dispersion is absent in this single molecule calculation. The energy levels of excited states are signed by straight lines in Fig. 4. It is shown that feature A is related to the lowest excited state, and other features are composed of multiple excited states. The calculated electron–hole wave functions for the four lowest excited states Ω_1–Ω_4 are depicted in Fig. 5(a). Each data point (x_{e}, x_{h}) in the figure represents the probability $|\Psi^{\mathrm{e}}(x_{\mathrm{e}}, x_{\mathrm{h}})|^2$ of finding the electron on site x_{e} and the hole on site x_{h}, and the darkness is related to the value of $|\Psi^{\mathrm{e}}(x_{\mathrm{e}}, x_{\mathrm{h}})|^2$ at point (x_{e}, x_{h}). The darker the point is, the bigger the probability of finding the electron and the hole at this point is. The excited states Ω_1–Ω_4 are shown

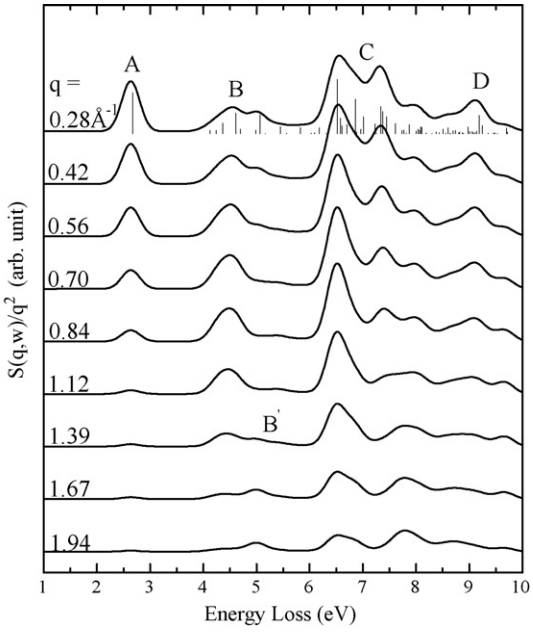

Fig. 4. The calculated IXS spectra for a single Py-SO molecule based on ZINDO/SCI.

to localize in a small fraction of the molecule. For example, the lowest excited state Ω_1 is mainly distributed among atoms 8–14 in the molecule.

The calculated optical absorption spectrum of the monomer is depicted in Fig. 6. The experimental absorption spectrum measured in DMF (dimethylformamide) [13] is shown in the inset for comparison. The calculated absorption spectrum is obtained with a broadening factor of 100 meV considering the temperature effect (room temperature) in the experiment. There are three main features at 2.64 eV, 4.6 eV and 5.0 eV in the calculated absorption spectrum, which can be closely compared with those in the calculated IXS spectra (Fig. 4). The feature at 2.64 eV is blue-shifted about 0.4 eV compared with the experimental absorption peak at 2.25 eV (553 nm) [13]. This could be attributed to the solvent effect neglected in our calculation.

2.2. Dimer

In order to reveal the nature of the dispersion with respect to increasing q, we first take two optimized molecules with the shortest separation in the Py-SO crystal. Fig. 3(b) shows the structure of the dimer with intermolecular separation of 3.67 Å. Following the atom labeling in the monomer in Fig. 3(a), the atom labeling in the dimer runs over molecule I then molecule II. The total Hamiltonian of the dimer is

$$H = H_1 + H_2 + H_{12} \tag{8}$$

where H_1 and H_2 are the Hamiltonians of molecule I and molecule II, respectively, and H_{12} describes the intermolecular interaction. There are several different models to treat the intermolecular interaction, such as the point-dipole approximation, the Frenkel exciton model, or the supermolecular approach. The point-dipole approximation works well only when the intermolecular distance is larger than the molecular size [22]. However, it is not the case for the dimer considered. The intermolecular interaction is purely Coulombic in the Frenkel exciton model, which can be applied to very large systems. It works well when the electron-exchange interaction is negligible; whereas it fails when charge transfer between molecules contributes significantly [23]. The supra-molecular approach considers both the Coulomb and the exchange interactions, as well as the charge-transfer effect. Nevertheless, the computation costs highly when the system is large.

Here, the dimer model is treated by the supermolecular approach. The hopping integrals in INDO are parameterized according to the inter-atomic orbital overlaps, which are evaluated by the Slater-type orbital (STO). And STOs possess an orbital radial dependence of $\exp(-\zeta r)$, which decays in large separation much slower than the commonly used Gaussian-type orbital $\exp(-\alpha r^2)$. This fact renders the suitability of INDO for treating intermolecular interaction. Indeed, Brédas et al. have extensively employed the INDO Hamiltonian in studying the intermolecular interaction effects in the cases of charge transfer and energy transfer [24]. Due to the intermolecular interaction

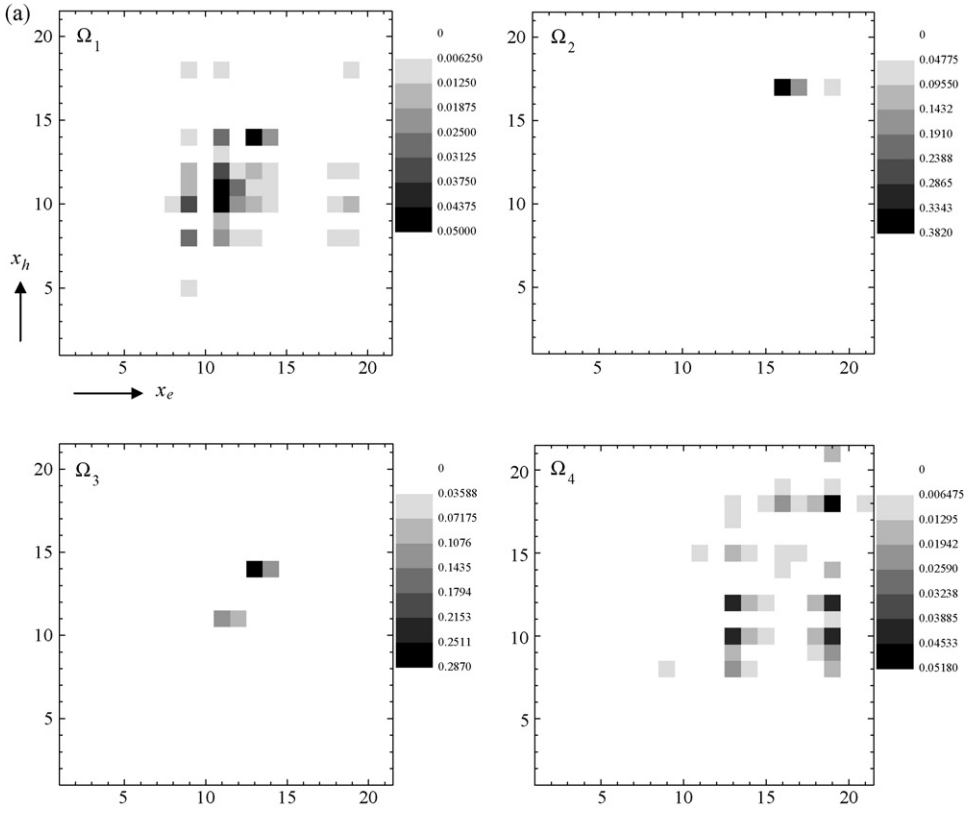

Fig. 5. (a) The electron–hole wave functions of the four lowest excited states in a single Py-SO molecule. The energies for the states Ω_1–Ω_4 are 2.635 eV, 3.292 eV, 3.567 eV and 4.088 eV. (b) The electron–hole wave functions of several lowest excited states in the dimer. The energies for the states $\Omega'_1 - \Omega'_4$ and Ω'_{CT} are 2.588 eV, 3.277 eV, 3.579 eV, 4.078 eV and 3.264 eV.

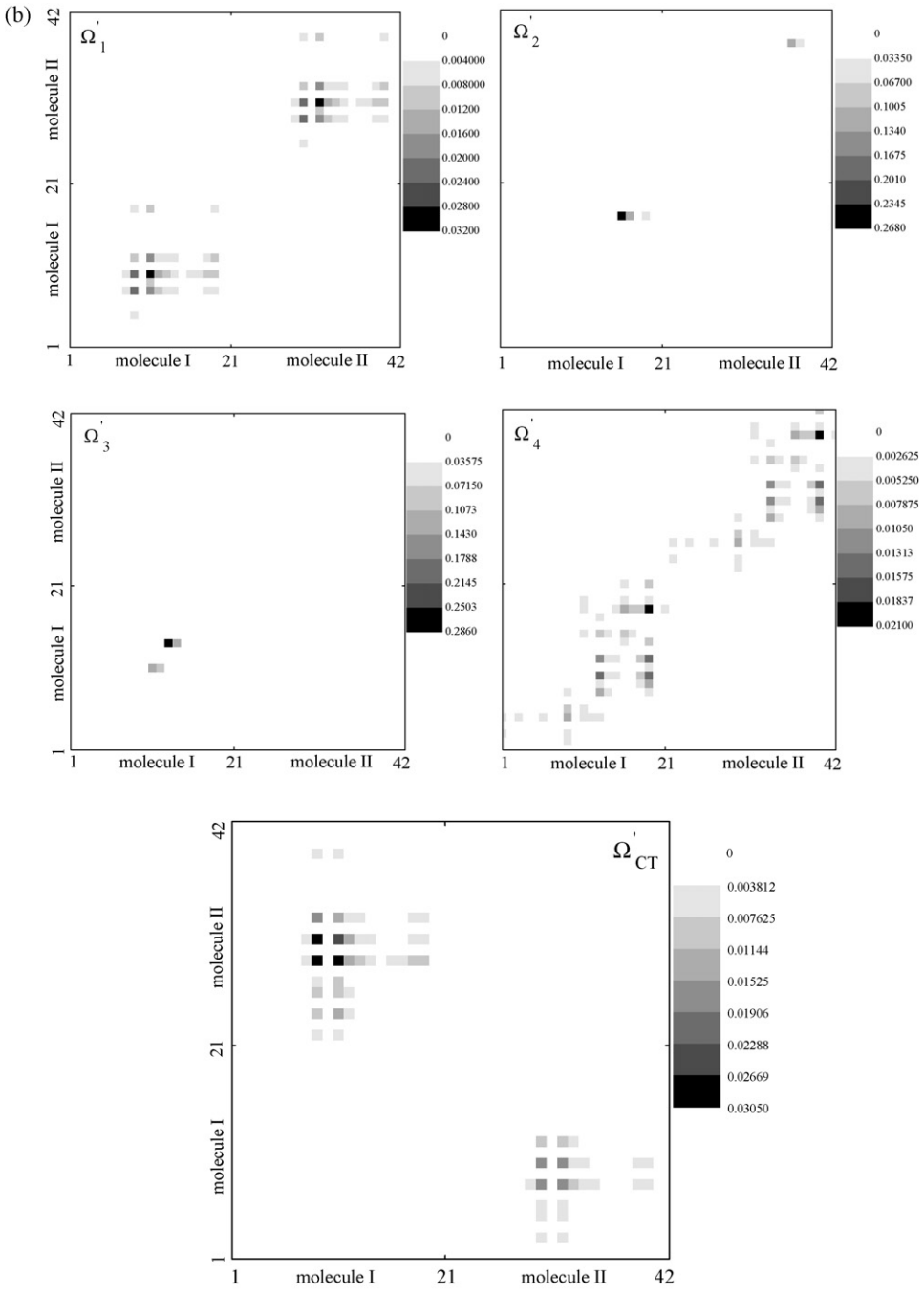

Fig. 5. (*Continued*).

in the dimer, every excited state in the monomer splits into a pair of states. In addition, there are pairs of intermolecular charge transfer (CT) type excited states. Each pair of the states are denoted as Ω' and Ω'', where Ω' corresponds to the state with stronger oscillator strength. The oscillator strength of various excited states of the dimer is shown in Fig. 7. The lowest excited states Ω'_1–Ω'_4 and Ω'_{CT} are pointed out. The calculated absorption spectrum of the dimer is depicted in the inset. The electron–hole wave functions of the lowest excited states Ω'_1–Ω'_4 and Ω'_{CT} for the dimer are shown in Fig. 5(b). For the excited states Ω'_1–Ω'_4, the electron–hole wave functions are similar to those of the corresponding states in the monomer as shown in Fig. 5(a). Each molecule retains its own electrons and electron exchange between molecules is negligible for this type of excitations. For the excited state Ω'_{CT}, electron exchange between molecules is involved. The lowest CT state is located at 3.26 eV. However, its oscillator strength is nearly zero with negligible contribution to the spectrum, which can be seen clearly from Fig. 7. Therefore, a simple Frenkel exciton model, which is common in molecular crystals and aggregated systems [25], can be applied to an aggregate of Py-SO molecules for further study.

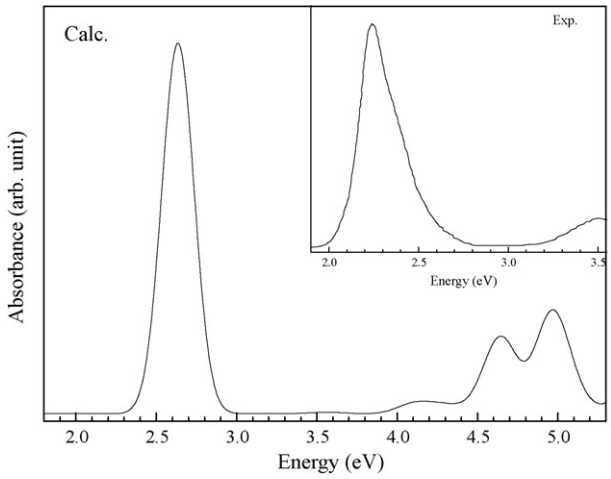

Fig. 6. The calculated absorption spectrum for a single Py-SO molecule. The experimental result is shown in the inset.

2.3. Aggregate

Since the energy dispersion in the IXS spectra is due to intermolecular interaction, we take an aggregate of optimized molecules with the strongest overlap in the Py-SO crystal into consideration. The structure of the aggregate is shown in Fig. 8. The adjacent inter-neighbor separation distances are 3.67 Å and 4.28 Å, respectively. The Frenkel exciton Hamiltonian for the aggregate is described as

$$H = \sum_{n,k} \varepsilon_{n,k} a^{+}_{n,k} a_{n,k} + \sum_{n>m,k,k'} J_{nk,mk'} a^{+}_{n,k} a_{m,k'} \tag{9}$$

where n is the site of molecule, $a_{n,k}$ ($a^{+}_{n,k}$) is the annihilation (creation) operator for molecular excitation k at site n, and the intermolecular excitation interaction J is calculated as

$$J_{nk,mk'} = \sum_{\mu_n,\mu_m} \rho^{g\to k}_{\mu_n} \rho^{g\to k'}_{\mu_m} [\mu_n \mu_n | \mu_m \mu_m] \tag{10}$$

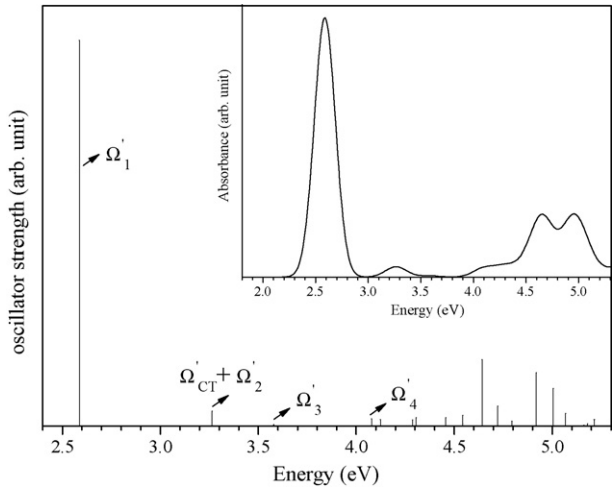

Fig. 7. The oscillator strength of various excited states of the dimer. The calculated absorption spectrum of the dimer is shown in the inset.

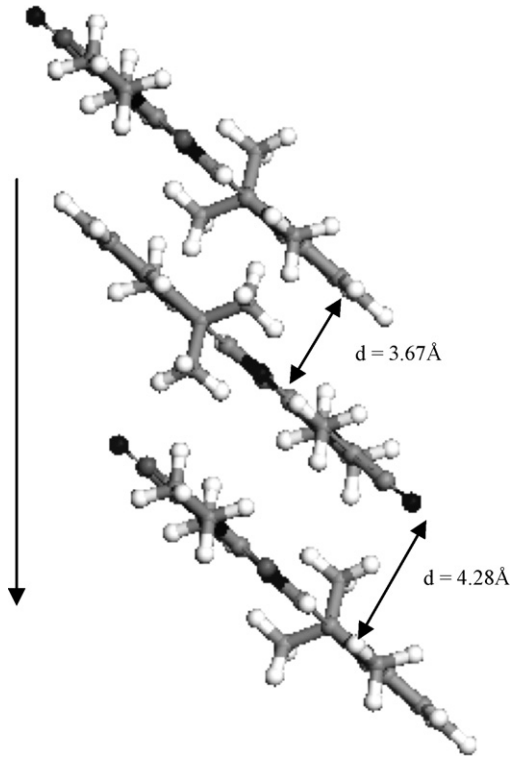

Fig. 8. The repeated unit of the aggregate with the strongest overlap in Py-SO crystal. There are two different separations of 3.67 Å and 4.28 Å between neighboring molecules.

where ρ is the transition density distribution expressed in atomic orbital basis μ for the nth molecule:

$$\rho^{g->k}_{\mu_n} = \int \psi_{n,g}(x_1, x_2, \ldots, x_N)\psi_{n,k}(x_1, x_2, \ldots, x_N) \times \mathrm{d}x_1\, \mathrm{d}x_2 \cdots \mathrm{d}x_{N-1} \tag{11}$$

where ψ is the many-body wave function of molecule n from single configuration interaction approach. $[\mu_n\mu_n \mid \mu_m\mu_m]$ is the intermolecular diagonal electronic Coulomb interaction. In the limit of large molecular separation, this interaction goes to the commonly used dipole–dipole interaction. We retain all the molecular excitations (indexed as k) from single molecule calculations to construct the exciton Hamiltonian, and the lth exciton wave function can be expressed as a linear combination of molecules (indexed as n) in the aggregate:

$$\Psi_l = \sum_{n,k} A^{l}_{n,k} |n, k\rangle \tag{12}$$

Here, $|n,k\rangle$ means the kth excited state of the nth molecule. The eigen equation of aggregate Hamiltonian is

$$\sum_{n,k} \langle m, k' | H | n, k\rangle A^{l}_{n,k} = E^{l} A^{l}_{m,k'} \tag{13}$$

The diagnonal elements are simply the single molecule excitation energy. The off-diagonal terms are $J_{m,k';n,k}$. Based on the exciton wave functions of the aggregate and the IXS data of the monomer, the dynamic structure factor for the aggregate can be

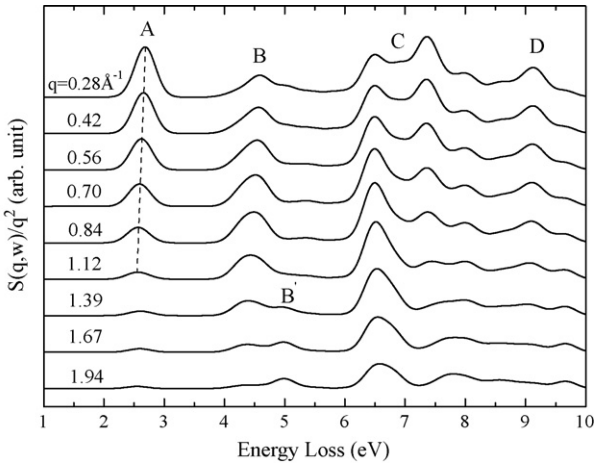

Fig. 9. The calculated IXS spectra for the aggregate. The bias shows a tendency of energy dispersion of the lowest exciton.

obtained:

$$\langle \Psi_0 \left| \sum_i e^{-i\vec{q}\cdot\vec{r}_i} \right| \Psi_l \rangle = \sum_{n,k} A^l_{n,k} \langle 0 \left| \sum_i e^{-i\vec{q}\cdot\vec{r}_i} \right| n,k \rangle \qquad (14)$$

where Ψ_0 is the aggregate ground state, which is a simple product of the monomer ground states in the Frenkel exciton theory. Eq. (14) can be easily evaluated through Eq. (7).

The momentum dependence of the dynamic structure factor for the aggregate is shown in Fig. 9. On the one hand, the calculated IXS spectra of the aggregate are quite similar to those of the monomer and retain the features A, B, B′, C and D in Fig. 4. On the other hand, energy dispersion of the lowest exciton appears in the aggregate calculation due to the consideration of intermolecular interaction. The momentum dependence of the energy position for the lowest exciton is listed in Table 1, which shows that the measured energy dispersion of 130 meV is well reproduced by our calculation. Fig. 10 depicts the momentum dependence of the integrated intensity for three main features. The overall agreements between the experiment and the calculation based on both the monomer and the aggregate are quite satisfactory. However, the calculated integrated intensities of high-energy features are overestimated as shown in Fig. 10(b) and (c). Actually, the aggregate calculation does give lower integrated intensity compared with the monomer calculation. We attribute the overestimation to the more delocalized nature of the high-energy excitons, which are less bound than the lowest exciton. Therefore, the monomer calculation would overestimate the on-site occupation, which in turn causes higher matrix element of IXS. Similarly, the aggregate calculation with a Frenkel exciton model would also overestimate the on-site occupation. In addition, the SCI approximation considers the correlation effect between electron and hole, but neglects the multi-particle correlation, which does not influence much the lower excitations, but could redistribute the momentum-dependent intensities for

Table 1
The calculated energy position of feature A in the aggregate when q varies from 0.28 Å^{-1} to 1.12 Å^{-1}

q (Å^{-1})	Energy (eV)	$E(0.28) - E(q)$ (eV)
0.28	2.682	0.000
0.42	2.657	0.025
0.56	2.623	0.059
0.70	2.590	0.092
0.84	2.567	0.115
1.12	2.562	0.120

The momentum dependence of energy dispersion is also given.

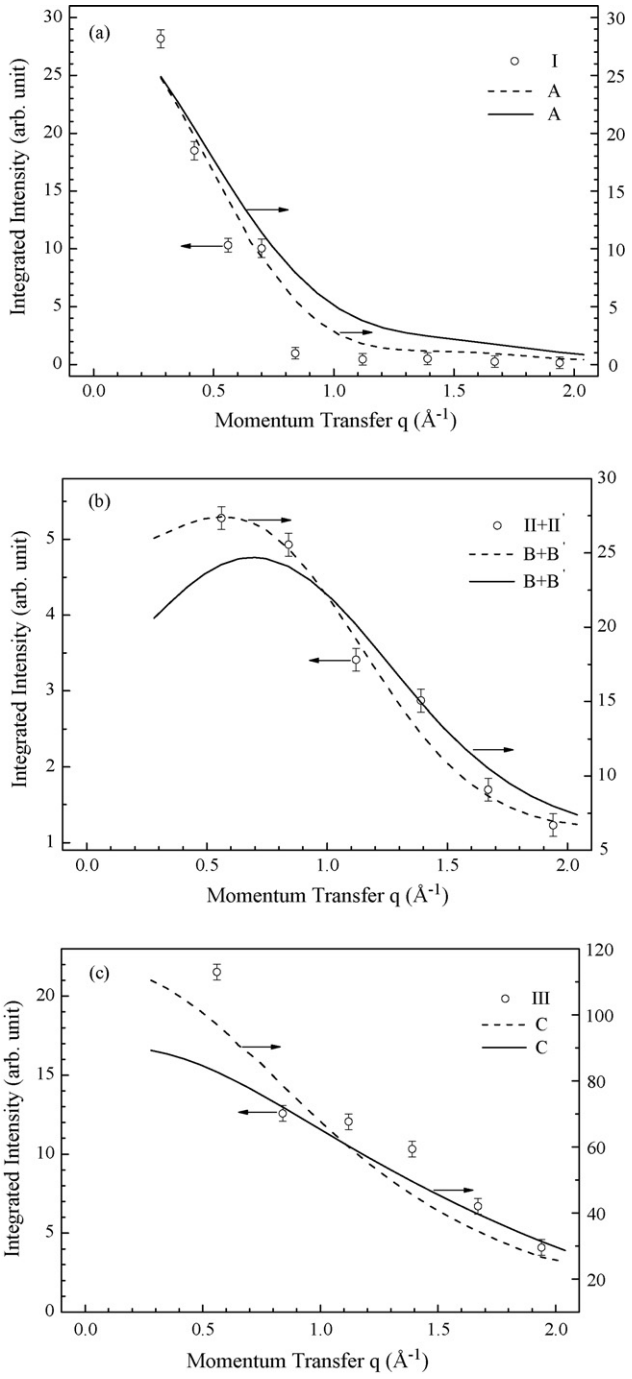

Fig. 10. Integrated intensity as a function of momentum in the experiment (open circle) and the calculation based on the monomer (dashed line) and the aggregate (solid line). (a) Features I and A integrated over [1.5 eV, 3.0 eV], (b) features II + II′ and B + B′ integrated over [4.0 eV, 5.5 eV], (c) features III and C integrated over [5.5 eV, 8.0 eV].

the higher energy features. The maximum intermolecular interaction J for the lowest exciton is calculated to be 55 meV. Therefore, the lowest exciton retains the property in a single molecule and extends over a fraction of the molecule. It is thus not surprise to see that even a single molecule calculation (Fig. 4) gives essentially the similar IXS features, except the dispersion behavior.

3. Summary

To summarize, we have carried out a quantum chemical simulation of IXS Spectra for an organic crystal of Py-SO. The localized nature of molecular exciton is revealed through electron–hole wave function. The calculated IXS spectra based on a single Py-SO molecule agree well with the experiment, except for the energy dispersion, which is due to intermolecular interaction. The lowest excited state is shown to localize in a small fraction of the molecule. Investigation on a dimer with the shortest separation in the Py-SO crystal shows that the intermolecular interaction is mainly Coulombic. CT states are found irrelevant to the optical spectra. Thus, a simple Frenkel exciton model is applied to an aggregate with the strongest overlap in the Py-SO crystal. Besides the energy position, the energy dispersion observed in the experiment is well reproduced by our calculation on the aggregate. The dispersion of the lowest exciton can give a good measure of the intermolecular interaction. The maximum coupling for the lowest exciton between molecules is found to be 55 meV. Therefore, the lowest exciton is of Frenkel type which extends over a small fraction of the molecule. Moreover, the calculated q-dependence of the integrated intensity of three main features is consistent with the experimental result. Besides the agreement with the experimental results, our calculations can give more information on the nature of both molecular excitations and excitons in Py-SO, which is useful to understand the electronic structures and optical properties of the material. It can also provide very useful guidance for designing new functional materials. For example, polymers attached by the molecular clusters of Py-SO molecules may present new optical behaviors due to the local property of the lowest exciton.

Acknowledgments

This work is supported by NSFC (Grant Nos. 10425420, 20433070, 10225418, 90401016) and Ministry of Science and Technology of China through 973 program (Grant Nos. 2002CB613406 and 2006CB0N0100), as well as the European Union 6th framework project MODECOM. The numerical computation is carried out in the Supercomputing Center of the Chinese Academy of Sciences.

References

[1] J.H. Burroughes, D.D.C. Bradley, A.R. Brown, R.N. Marks, K. Mckay, R.H. Friend, P.L. Burn, A. Kraft, A.B. Holmes, Nature 347 (1990) 539;
Q. Pei, G. Yu, C. Zhang, Y. Yang, A.J. Heeger, Science 269 (1995) 1086.
[2] N.C. Greenham, R.H. Friend, Solid State Phys. 49 (1995) 1.
[3] H. Horowitz, F. Garnier, A. Yassar, R. Hajlaoui, F. Kouki, Adv. Mater. 8 (1996) 52.
[4] N.S. Sariciftci, L. Smilowitz, A.J. Heeger, F. Wudl, Science 258 (1992) 1474;
J.J.M. Halls, C.A. Walsh, N.C. Greenham, E.A. Marseglia, R.H. Friend, S.C. Moratti, A.B. Holmes, Nature 376 (1995) 498.
[5] D. Fichou, J.M. Nunzi, F. Charra, N. Pfeffer, Adv. Mater. 6 (1994) 64.
[6] J. Cornil, D.A. dos Santos, X. Crispin, R. Silbey, J.L. Brédas, J. Am. Chem. Soc. 120 (1998) 1289;
J. Cornil, D. Beljonne, J.-P. Calbert, J.L. Brédas, Adv. Mater. 13 (2001) 1053;
S. Tretiak, A. Saxena, R.L. Martin, A.R. Bishop, J. Phys. Chem. B 104 (2000) 7029.
[7] M. Knupfer, T. Pichler, M.S. Golden, J. Fink, M. Murgia, R.H. Michel, R. Zamboni, C. Taliani, Phys. Rev. Lett. 83 (1999) 1443;
E. Zojer, M. Knuper, Z. Shuai, J.L. Brédas, J. Fink, G. Leising, J. Phys.: Condens. Matter 12 (2000) 1753;
M. Knupfer, J. Fink, E. Zojer, G. Leising, J.L. Brédas, Phys. Rev. B 61 (2000) 1662;
M. Knupfer, J. Fink, Synth. Met. 141 (2004) 21.
[8] W. Schülke, J. Phys.: Condens. Matter 13 (2001) 7557.
[9] E.D. Isaacs, P.M. Platzman, P. Metcalf, J.M. Honig, Phys. Rev. Lett. 76 (1996) 4211.
[10] W. Schülke, H. Schulte-Schrepping, J.R. Schmitz, Phys. Rev. B 47 (1993) 12426.
[11] W.A. Caliebe, J.A. Soininen, E.L. Shirley, C.-C. Kao, K. Hamalainen, Phys. Rev. Lett. 84 (2000) 3907.
[12] K. Yang, L.P. Chen, Y.Q. Cai, N. Hiraoka, S. Li, J.F. Zhao, D.W. Shen, H.F. Song, H. Tian, L.H. Bai, Z.H. Chen, Z.G. Shuai, D.L. Feng, Phys. Rev. Lett. 98 (2007) 036404.
[13] H.F. Song, K.C. Chen, H. Tian, Dyes Pigments 67 (2005) 1.
[14] AMPAC, version 5.0, Semichem, Shawnee, KS, 1994.
[15] J. Ridley, M.C. Zerner, Theor. Chim. Acta 32 (1973) 111;
M.C. Zerner, G.H. Loew, R.F. Kichner, U.T. Mueller-Westerhoff, J. Am. Chem. Soc. 102 (1980) 589.
[16] N. Mataga, K. Nishimoto, Z. Phys. Chem. 13 (1957) 140.
[17] G.R. Hutchison, M.A. Ratner, T.J. Marks, J. Phys. Chem. A 106 (2001) 10596.
[18] A. Dreuw, M. Head-Gordon, Chem. Rev. 105 (2005) 4009.
[19] A. Kohler, D.A. dos Santos, D. Beljonne, Z. Shuai, J.L. Brédas, R.H. Friend, S.C. Moratti, A.B. Holmes, A. Kraus, K. Mullen, Nature 392 (1998) 903;
J.L. Brédas, J. Cornil, D. Beljonne, D.A. dos Santos, Z. Shuai, Acc. Chem. Res. 32 (1999) 267.
[20] In Ref. [12], an anti-symmetrized two-particle wave function has been employed. We are grateful to Dr. Lorenz Romaner from Technical University of Graz, Austria, who reminds us that the un-symmetrized form of Eq. (2) is more physically meaningful (see Ref. [19]), though it does not alter any localization characterization of molecular excitation.
[21] S. Doniach, P.M. Platzman, J.T. Yue, Phys. Rev. B 4 (1971) 3345.
[22] Z.G. Soos, G.W. Hayden, P.C.M. McWilliams, S. Etemad, J. Chem. Phys. 93 (1990) 7439;
S. Marguet, D. Markovitsi, P. Millié, H. Sigal, S. Kumar, J. Phys. Chem. B 102 (1998) 4697.
[23] D. Beljonne, J. Cornil, R. Silbey, P. Millié, J.L. Brédas, J. Chem. Phys. 112 (2000) 4749.
[24] J.L. Brédas, D. Beljonne, V. Coropceanu, J. Cornil, Chem. Rev. 104 (2004) 4971.
[25] M. Pope, C.E. Swenberg, Electronic Processes in Organic Crystals, Oxford, New York, 1982;
E.I. Rashba, M.D. Sturge (Eds.), Excitons, North-Holland, Amsterdam, 1982;
V.B. Broude, E.I. Rashba, E.F. Sheka, Spectroscopy of Molecular Excitons, Springer, Berlin, 1985;
E.A. Silinsh, V. Čápek, Organic Molecular Crystals, American Institute of Physics, New York, 1994.